







Article

Acidogenesis of Pentose Liquor to Produce Biohydrogen and Organic Acids Integrated with 1G–2G Ethanol Production in Sugarcane Biorefineries

Guilherme Peixoto ^{1,2} , Gustavo Mockaitis ^{3,4} , Wojtyła Kmiecik Moreira ⁴, Daniel Moureira Fontes Lima ⁵ , Marisa Aparecida de Lima ², Filipe Vasconcelos Ferreira ⁴, Lucas Tadeu Fuess ^{4,*} , Igor Polikarpov ²  and Marcelo Zaiat ⁴ 

- ¹ Department of Engineering of Bioprocesses and Biotechnology, School of Pharmaceutical Sciences, São Paulo State University (UNESP), São Paulo 14800-903, SP, Brazil; guilherme.peixoto@unesp.br
 - ² Molecular Biotechnology Group, São Carlos Physics Institute, University of São Paulo (IFSC/USP), São Carlos 13566-590, SP, Brazil; marisalima2000@yahoo.com.br (M.A.d.L.); ipolikarpov@ifsc.usp.br (I.P.)
 - ³ Interdisciplinary Research Group On Biotechnology Applied to the Agriculture and the Environment (GBMA), School of Agricultural Engineering (FEAGRI), University of Campinas (UNICAMP), Av. Candido Rondon, 501–Cidade Universitária, São Paulo 13083-875, SP, Brazil; gusmock@unicamp.br
 - ⁴ Biological Processes Laboratory, São Carlos School of Engineering, University of São Paulo (EESC/USP), São Carlos 13563-120, SP, Brazil; wojtyla.kmiecik@gmail.com (W.K.M.); filipevasconcelos@usp.br (F.V.F.); zaiat@sc.usp.br (M.Z.)
 - ⁵ Department of Civil Engineering, Federal University of Sergipe (UFS), São Cristóvão 49107-230, SE, Brazil; danielmfl@academico.ufs.br
- * Correspondence: lt.fuess@usp.br; Tel.: +55-(16)-3373-8360



Citation: Peixoto, G.; Mockaitis, G.; Moreira, W.K.; Lima, D.M.F.; de Lima, M.A.; Ferreira, F.V.; Fuess, L.T.; Polikarpov, I.; Zaiat, M. Acidogenesis of Pentose Liquor to Produce Biohydrogen and Organic Acids Integrated with 1G–2G Ethanol Production in Sugarcane Biorefineries. *Waste* **2023**, *1*, 672–688. <https://doi.org/10.3390/waste1030040>

Academic Editors: Vassilis Athanasiadis and Dimitris P. Makris

Received: 3 July 2023
Revised: 21 July 2023
Accepted: 31 July 2023
Published: 5 August 2023



Copyright: © 2023 by the authors. Licensee MDPI, Basel, Switzerland. This article is an open access article distributed under the terms and conditions of the Creative Commons Attribution (CC BY) license (<https://creativecommons.org/licenses/by/4.0/>).

Abstract: Second-generation (2G) ethanol production has been increasingly evaluated, and the use of sugarcane bagasse as feedstock has enabled the integration of this process with first-generation (1G) ethanol production from sugarcane. The pretreatment of bagasse generates pentose liquor as a by-product, which can be anaerobically processed to recover energy and value-added chemicals. The potential to produce biohydrogen and organic acids from pentose liquor was assessed using a mesophilic (25 °C) upflow anaerobic packed-bed bioreactor in this study. An average organic loading rate of 11.1 g COD·L^{−1}·d^{−1} was applied in the reactor, resulting in a low biohydrogen production rate of 120 mL·L^{−1} d^{−1}. Meanwhile, high lactate (38.6 g·d^{−1}), acetate (31.4 g·d^{−1}), propionate (50.1 g·d^{−1}), and butyrate (50.3 g·d^{−1}) production rates were concomitantly obtained. Preliminary analyses indicated that the full-scale application of this anaerobic acidogenic technology for hydrogen production in a medium-sized 2G ethanol distillery would have the potential to completely fuel 56 hydrogen-powered vehicles per day. An increase of 24.3% was estimated over the economic potential by means of chemical production, whereas an 8.1% increase was calculated if organic acids were converted into methane for cogeneration (806.73 MWh). In addition, 62.7 and 74.7% of excess organic matter from the 2G ethanol waste stream could be removed with the extraction of organic acid as chemical commodities or their utilization as a substrate for biomethane generation, respectively.

Keywords: sugarcane bagasse; pentose liquor; dark fermentation; biohydrogen; organic acids; biorefinery

1. Introduction

Brazilian sugarcane mills are migrating from old concepts of sugar and ethanol production to a new concept of biorefinery. This concept aims to produce not only biofuels but also electricity, food, and other products that use renewable sources from sugarcane biomass [1–3]. One of the main actions to consolidate the biorefinery concept is the implementation of second-generation (2G) ethanol production integrated with first-generation (1G) plants. This industrial concept intends to use surplus bagasse that is currently used as

fuel in cogeneration systems, to produce lignocellulosic ethanol (2G) instead [4]. The utilization of this remaining biomass plays a fundamental role in the biorefinery yield because 1 ton of sugarcane generates 280 kg of bagasse [5], which is very significant considering the production of 610 million tons of sugarcane [6] in the 2022/2023 harvest.

The implementation of 2G ethanol production can improve process sustainability and also ethanol production [7,8]. In this process, the bagasse is pretreated to obtain a solid fraction that is rich in cellulose, while hemicellulose is mainly hydrolyzed to pentoses (pentose liquor). The cellulose fraction obtained from this pretreatment can be enzymatically hydrolyzed to feed the 2G ethanol-producing process, and pentose liquor remains a by-product of the process. Although ethanol production is the natural destination of the hexoses (C6) fraction, the processing of pentose liquor is still not well defined, and alternatives must be studied for the application of this stream. For instance, opportunities for fermenting pentoses to obtain ethanol have been massively studied [9,10]; however, selecting efficient pentose fermenters is still challenging.

The xylose-rich nature of pentose liquor characterizes it as a highly suitable substrate for biohydrogen and organic acid production in acidogenic bioreactors because this process depends primarily on carbohydrate-rich substrates [11,12]. Hydrogen is a renewable clean energy carrier when biomass and its by-products are used as raw materials in fermentation. The biological production of hydrogen from residues and wastewater is less energy intensive and is less expensive than methane steam reforming and electrolysis [11–14]. Moreover, various organic acids and other compounds with different applications (foods, pharmaceuticals, and chemicals) can be generated during the biological production of hydrogen. Most studies have reported that biohydrogen production generates intermediates such as acetic acid, propionic acid, butyric acid, succinic acid, formic acid, butanediol, and acetone [15–20]. These compounds are of special interest because of their high market value [21,22], especially butyric and lactic acid, which are used as precursors of industrial thermoplastics [23] and biodegradable polymers [24,25]. Although only a few studies have addressed hydrogen and organic acid production using sugarcane bagasse (SCB) hydrolysate [26–30], several studies have used pure xylose as a substrate for the production of biohydrogen [31–39], indicating a gap for exploitation within the context of dark fermentation studies. Furthermore, most researchers have used batch reactors in contrast with the few studies conducted in continuous bioreactors. Neither xylose nor SCB hydrolysate have been used in upflow anaerobic packed-bed reactors, which have generally yielded high biohydrogen productivity [40–44].

This study assessed the potential application of sugarcane bagasse-derived pentose liquor as a source of biohydrogen and organic acids in a continuous packed-bed bioreactor, characterizing an alternative to add value to a voluminous by-product which will be inevitably available in integrated 1G-2G sugarcane biorefineries in coming years. A dual approach based on an experimental assessment followed by a scenarization-based exercise through a simple process application analysis in a medium-sized distillery (milling capacity of $500 \text{ ton} \cdot \text{h}^{-1}$) was carried out, providing the bases to understand the potential of pentose liquor as a substrate for biotechnological applications.

2. Materials and Methods

2.1. Bioreactor and Support Material

The upflow anaerobic packed-bed reactor (UAPBR) was built in tubular acrylic with a length-to-diameter (L/D) ratio of 9.4, considering a total height of 750 mm and a working volume of 2.370 L. The bioreactor's bed region was randomly filled with recycled low-density polyethylene (LDPE) pellets to support cell attachment, similar to previous experiments with real wastewater [43–45]. Cylinder-shaped particles with a mean diameter of 12.7 mm and ca. 30 mm in height were used with specific gravity and a surface area of $0.96 \text{ g} \cdot \text{cm}^{-3}$ and $7.94 \text{ m}^2 \cdot \text{g}^{-1}$, respectively. A total of $295 \text{ g LDPE} \cdot \text{L}^{-1}$ was used to build the bed zone, resulting in a bed porosity of 55%. The packed bed occupied 66% of the total volume. A schematic diagram of the reactor is shown in Figure 1.

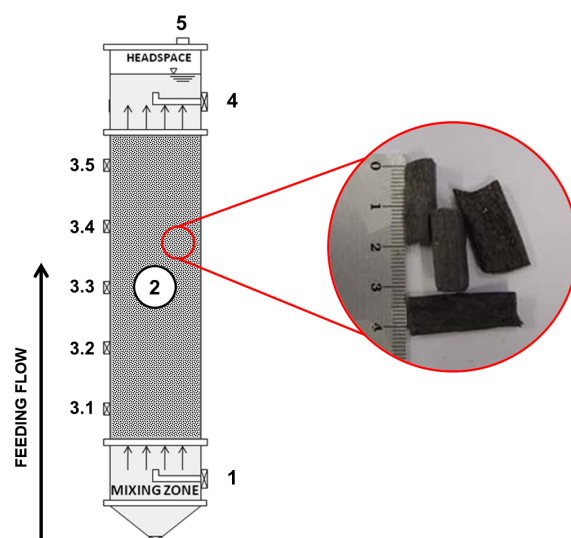


Figure 1. Sketch of the upflow anaerobic packed-bed reactor and details of the LDPE pellets. Legend: 1—inlet port, 2—packed bed, 3.1–3.5—sampling ports, 4—outlet port (liquid phase), 5—outlet port (biogas).

2.2. Substrates

The UAPBR was fed with two different substrates in distinct operating periods, namely, a xylose-based lab-made wastewater (experimental condition I) and pentose liquor derived from 2G ethanol production (experimental condition II), as indicated in Figure 2. The former was prepared using 99.9% pure D-(+)-Xylose (Sigma-Aldrich®, San Luis, MO, USA), whilst pentose liquor was obtained from the processing of residual SCB collected from a Brazilian sugarcane mill. Bagasse was subjected to physicochemical pretreatment (121 °C and 1.1 atm) utilizing a mass ratio of solid (g dry weight) to liquor (g) at 1:10 with 2% sulfuric acid (H_2SO_4) (*v/v*) for 60 min [46]. This pretreatment resulted in a hydrolysate with an organic matter concentration in terms of COD (chemical oxygen demand) of $14 \text{ g} \cdot \text{L}^{-1}$. Prior to feeding the bioreactor, the hydrolysate was neutralized with sodium hydroxide (NaOH) and diluted with tap water to obtain a COD of approximately $2 \text{ g} \cdot \text{L}^{-1}$. The compositional characteristics of the wastewater utilized in both experimental conditions are shown in Table 1.

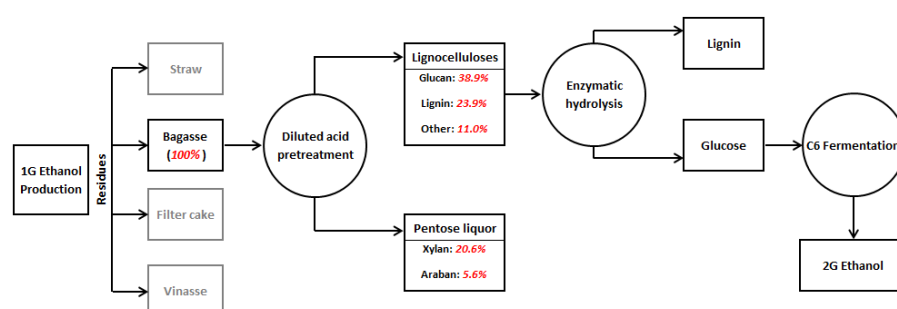


Figure 2. Processing of sugarcane bagasse to produce second generation ethanol. Sugarcane bagasse constituents by Aguilar et al. [46].

Table 1. Compositional characterization of the wastewater used in reactor feeding.

Parameters	Xylose-Based Wastewater	Pentose Liquor
Total carbohydrates ($\text{mg} \cdot \text{L}^{-1}$)	1495 ± 733	1459 ± 440
Xylose (%)	99.9	82.4
Arabinose (%)	—	7.12
Rhamnose (%)	—	6.14
Glucose (%)	—	1.58
pH	6.7 ± 0.1	5.9 ± 0.1

2.3. Experimental Procedure

Bioreactor inoculation was carried out prior to experimental conditions I and II and consisted of the natural fermentation of xylose and pentose liquor, respectively. The natural fermentation was performed by exposing 30 L of each medium for 3 days to the atmosphere at ca. 25 °C. In previous studies, such as those published elsewhere [16,40,41], this procedure yielded mainly microorganisms similar to *Clostridium* sp. (91%), *Klebsiella* sp. (97%), and *Enterobacter* sp. (93%), which are directly related to hydrogen and organic acid production [41]. Naturally fermented substrates were recirculated into the UAPBR for 7 days [16] as a strategy to promote the attachment of microorganisms to the packed bed, after which a continuous operation was started. The volumetric flow rate of the bioreactor feed was maintained at ca. 1.19 L·h⁻¹ using a positive displacement pump (Concept Plus, ProMinent Brasil Ltd.a., São Bernardo do Campo, Brazil), resulting in a hydraulic retention time (HRT) of 2 h. The operating temperature was controlled at 25 ± 1 °C in a thermostatic chamber (410-DRE, Nova Ética, Vargem Grande Paulista, Brazil). In condition I, xylose was used as the only substrate for 36 days, whilst pentose liquor was evaluated as the substrate for 39 days in condition II. The pH of both substrates (lab-made and real wastewater) was maintained at ca. 6.0 by dosing with NaOH (500 mg·L⁻¹) or hydrochloric acid (HCl) (10 mol·L⁻¹) solutions. Additionally, both media were supplemented with a macro and micronutrient solution containing (in mg·L⁻¹): CH₄N₂O (7.7), NiSO₄·6H₂O (0.15), FeSO₄·7H₂O (2.5), FeCl₃·6H₂O (0.25), CoCl₂·2H₂O (0.04), CaCl₂·6H₂O (2.06), SeO₂ (0.036), KH₂PO₄ (1.3), KHPO₄ (5.36), and Na₂HPO₄·2H₂O (2.76).

2.4. Monitoring Procedure and Analytical Methods

Liquid phase monitoring was based on periodic measurements of the pH, COD, and concentrations of the total carbohydrates, organic acids, and solvents. pH and COD were determined according to the Standard Methods for the Examination of Water and Wastewater [47]. Potentiometric measurements (pH) were carried out using a pH meter with a standard glass electrode (Digimed Instrumentação Analítica, São Paulo, Brazil). Total carbohydrates were measured as proposed by Dubois et al. [48], whilst organic acids and solvents were analyzed with a high-performance liquid chromatography (HPLC) system (Shimadzu Scientific Instruments, Kyoto, Japan) using the same configuration and protocols described elsewhere [49].

Gas phase monitoring was carried out by measuring both the biogas flow rate (BFR) and composition. BFR was obtained by directly coupling a gas meter (MilliGascounter-1 V30, Dr.-Ing. Ritter Apparatebau GMBH & Co. KG, Bochum, Germany) to the headspace of the reactor. The biogas composition in terms of hydrogen (H₂), nitrogen (N₂), methane (CH₄), and carbon dioxide (CO₂) was carried out using a gas chromatography set (GC-2010) equipped with a thermal conductivity detector (GC/TCD; Shimadzu Scientific Instruments, Kyoto, Japan) and argon as the carrier gas, as described elsewhere [50]. Gas samples were collected from UAPBR's headspace with 1000 µL-insulin syringes equipped with Teflon body two-way valves (Supelco[®] Analytical—Sigma-Aldrich, Bellefonte, PA, USA).

2.5. Scenario Assessment

Four different scenarios, namely, 1 to 4, were considered for a medium-sized 2G ethanol plant (milling capacity of 500 ton·h⁻¹), providing a preliminary analysis of pentose liquor as raw material for producing bioenergy and biochemicals. Scenarios 1 and 2 did not include pentose as raw material, whilst scenarios 3 and 4 considered the utilization of pentoses for the energy recovery and/or generation of value-added products. In Scenario 1, 50% of SCB was considered to be used for 2G ethanol production, with the remaining fraction used in the cogeneration of electricity and steam. In Scenario 2, 100% of SCB was directed to 2G ethanol production. In Scenario 3, 2G ethanol was produced with the utilization of all available SCB. Additionally, hydrogen and volatile organic acids (VOA) were derived from pentose liquor. In Scenario 4, 2G ethanol, hydrogen, and organic acids

were produced. In this last scenario, organic acid consumption in biomethane production for cogeneration was considered despite the use of chemicals, as reported in Scenario 3.

3. Results and Discussion

3.1. Biohydrogen Production

Biogas generation profiles obtained with xylose-based wastewater and pentose liquor are depicted in Figure 3, showing distinct patterns according to the type of substrate. In experimental condition I (xylose as the substrate), biogas production reached $193.8 \text{ mL}\cdot\text{h}^{-1}$ ($4.65 \text{ L}\cdot\text{d}^{-1}$) on day 10. This production peak was followed by continuous decay until the end of the operation (Figure 3A). This drop in biogas generation has also been observed in previous studies regarding hydrogen production from carbohydrates [40–42] and complex wastewaters [44,51]. A coherent explanation can be found in the major growth of homoacetogenic organisms, which are capable of using the Wood–Ljungdahl pathway because the applied specific organic load decreased with the increase in the biomass in the packed-bed reactor [52,53]. The homoacetogenic pathway explains the biogas production decrease because both H_2 and CO_2 produced by hydrogen-producing bacteria (HPB) were converted into acetate, as demonstrated in Reaction (1) [54]. Numerous studies dealing with the dark fermentation of sugarcane-derived substrates, namely, vinasse, molasses, and juice, have reported the occurrence of homoacetogenesis when applying mesophilic temperature conditions [19,55–58], which supports this hypothesis. Homoacetogenic bacteria belonging to genera *Moorella*, *Oxobacter*, and *Sporomusa*, as well as to the family *Lachnospiraceae*, were identified in vinasse-fed reactors [19,59,60]. Some clostridial groups [61], as well as some sulfate-reducing bacteria belonging to the genus *Desulfotomaculum* [62], are also capable of utilizing H_2 and CO_2 .

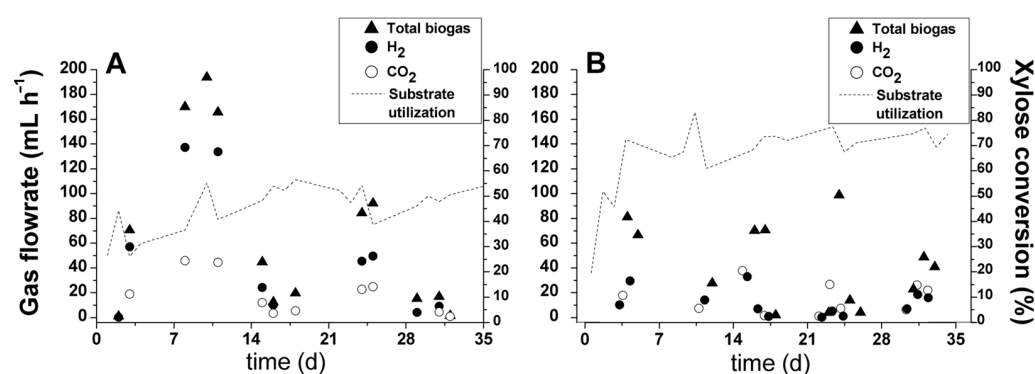
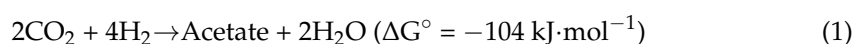


Figure 3. Biogas flowrate and composition and substrate utilization in experimental conditions (A) I (xylose-based wastewater) and (B) II (pentose liquor).

The mean biogas production rates obtained in conditions I and II were $0.026 \text{ L}\cdot\text{L}^{-1}\cdot\text{h}^{-1}$ ($624 \text{ mL}\cdot\text{L}^{-1}\cdot\text{d}^{-1}$) and $0.017 \text{ L}\cdot\text{L}^{-1}\cdot\text{h}^{-1}$ ($408 \text{ mL}\cdot\text{L}^{-1}\cdot\text{d}^{-1}$), respectively. The volumetric hydrogen production rate (VHPR) followed the same trend, with values of 0.016 ($384 \text{ mL}\cdot\text{L}^{-1}\cdot\text{d}^{-1}$) and $0.005 \text{ L}\cdot\text{h}^{-1}\cdot\text{L}^{-1}$ ($120 \text{ mL}\cdot\text{L}^{-1}\cdot\text{d}^{-1}$) observed in experimental conditions I and II, respectively. The main reason for a higher hydrogen production rate in the bioreactor processing xylose was the production peak reported at the beginning of the operation (days 8–11). This behavior could be explained considering that the substrate in condition I consisted only of readily available xylose, which could potentially contribute to a faster and more efficient biomass adaptation [63].

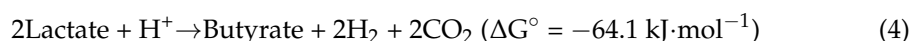
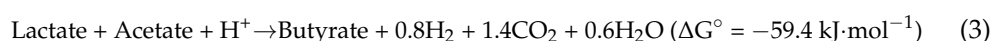
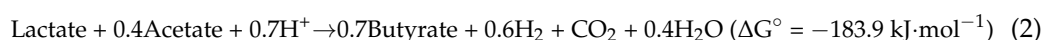
By contrast, experimental condition II contained a mixture of pentoses (xylose, arabinose, and rhamnose; Table 1). These different carbon sources and the presence of furfural and acetic acid could be responsible for lower hydrogen production rate at the beginning of the bioreactor operation. In the study by Aguilar et al. [46], the sugarcane bagasse

subjected to the same diluted acid pretreatment released approximately $1.2 \text{ g}\cdot\text{L}^{-1}$ of furfural and $4.5 \text{ g}\cdot\text{L}^{-1}$ of acetic acid, which are considered toxic to fermentation in these ranges [46,64]. However, the hydrolysate generated in this study was diluted by a factor of 7 (COD decreased from 13,989 to 1989 $\text{mg}\cdot\text{L}^{-1}$) before its utilization in the bioreactor, which consequently resulted in lower concentrations of both constituents. Thus, the best explanation for the worst performance in biohydrogen production in condition II was the lower rate of biomass adaptation. Nevertheless, after 11 days of operation, the highest peak of substrate utilization (83.2%) was noticed in this experimental condition (pentose-containing hydrolysate). According to the biogas profile in Figure 3B, xylose was not utilized for hydrogen production. Rather, this substrate was diverted for the production of soluble metabolites. Overall, in both conditions, the reported efficiency in xylose conversion (Figure 3A,B) was considered high because UAPBR was operated at a short hydraulic retention time (2 h).

Because the pentose liquor derives from sugarcane, it is pertinent to compare the obtained results with those found in the dark fermentation of other sugarcane-derived substrates, focusing on fixed-film reactors. Overall, the VHPR observed in condition II ($120 \text{ mL}\cdot\text{L}^{-1}\cdot\text{d}^{-1}$) exceeded only the value reported by Ferraz Jr. et al. [51], who achieved a mean VHPR of $84 \text{ mL}\cdot\text{L}^{-1}\cdot\text{d}^{-1}$ while processing vinasse in an LDPE-filled UAPBR at mesophilic conditions (25°C). Using the same type of substrate and reactor but at thermophilic conditions (55°C), much better results were reported, namely, $526.8 \text{ mL}\cdot\text{L}^{-1}\cdot\text{d}^{-1}$ [65], $761.7 \text{ mL}\cdot\text{L}^{-1}\cdot\text{d}^{-1}$ [43] and $1604 \text{ mL}\cdot\text{L}^{-1}\cdot\text{d}^{-1}$ [44]. Changing the bed conformation, i.e., replacing the random packing by orderly placing the support media further produced even better results, with VHPR reaching $2074 \text{ mL}\cdot\text{L}^{-1}\cdot\text{d}^{-1}$ [66] and $3477 \text{ mL}\cdot\text{L}^{-1}\cdot\text{d}^{-1}$ [67] while still considering vinasse as the substrate and temperature conditions. Comparing the results obtained herein with the utilization of vinasse is pertinent because both the pentose liquor and vinasse are highly complex materials. The use of molasses, a much simpler carbohydrate-rich sugarcane-derived by-product, led to much higher VHPR values, reaching $4504 \text{ mL}\cdot\text{L}^{-1}\cdot\text{d}^{-1}$ [68] and $8479 \text{ mL}\cdot\text{L}^{-1}\cdot\text{d}^{-1}$ [69]. Apart from the temperature and support material arrangement differences, in most of the comparative studies, much higher organic loading rate (OLR) levels were used ($>50 \text{ g COD}\cdot\text{L}^{-1}\cdot\text{d}^{-1}$) compared to the one applied in the UAPBR ($11.1 \text{ g COD}\cdot\text{L}^{-1}\cdot\text{d}^{-1}$), which could explain the high discrepancy among the VHPR values. Future studies with pentose liquor should focus on optimizing the OLR, as carried out for vinasse [65,66] and molasses [68].

3.2. Organic Acid Production

The distribution of soluble metabolites in experimental conditions I and II showed a higher amount of organic acids and solvents in the latter (Figure 4D,E). It is likely that hydrolysate compounds, especially the macro and micronutrients released during the hydrolysis of SCB, stimulated the metabolism of immobilized bacteria toward soluble metabolite production. Lactate was produced in large quantities in both experimental conditions. One plausible explanation for its high concentration is the short HRT (2 h) utilized in the bioreactor operation. The reduced HRT could have led to the accumulation of lactic acid because the reaction time was not sufficient to convert lactate and acetate to butyrate and hydrogen. This hypothesis is supported by the hydrogen profiles (Figure 3A,B) and the metabolic pathway suggested elsewhere [70], as demonstrated in Reactions (2)–(4). The results observed during the dark fermentation of other sugarcane-derived substrates, such as vinasse [20,66,67,71] and molasses [68,69,72], also corroborate this hypothesis because in all cases, lactate was identified as the primary precursor of biohydrogen and butyrate.



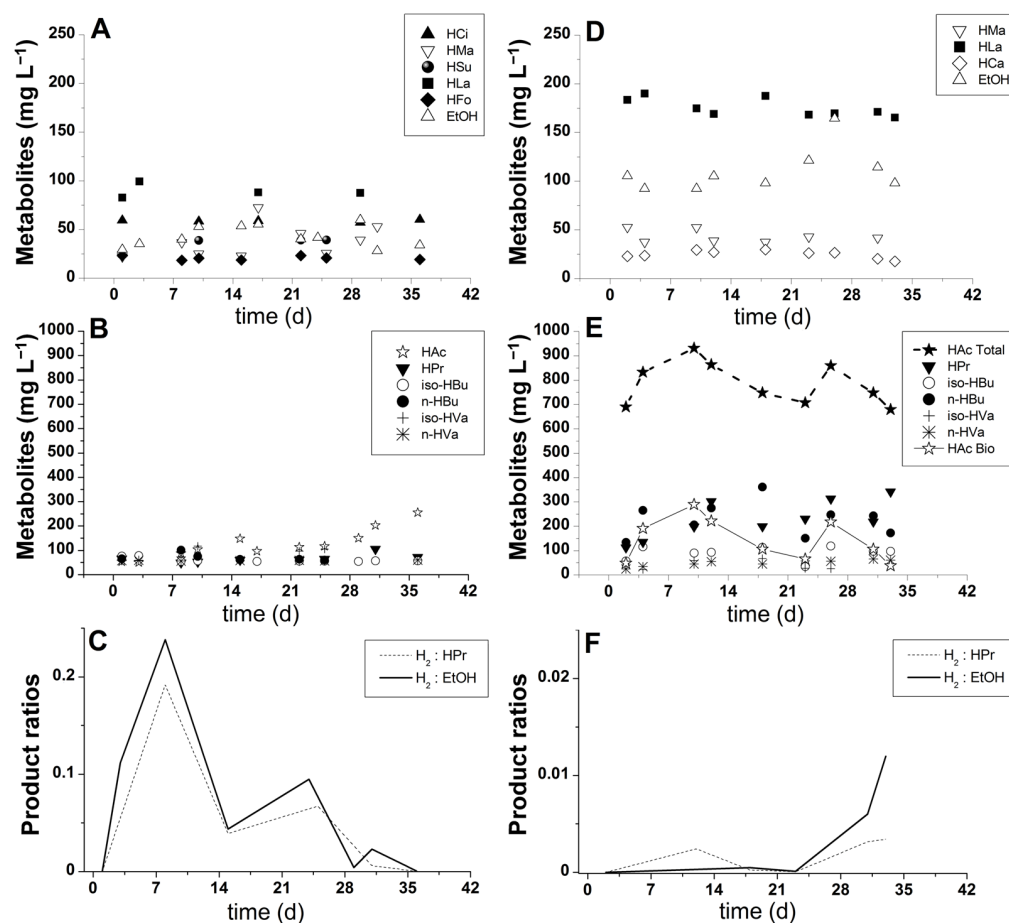


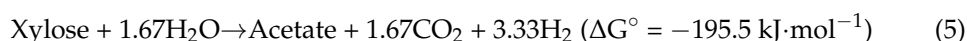
Figure 4. Condition I (xylose-based wastewater): (A,B) soluble phase products and (C) hydrogen-to-propionate (H_2 :HPPr) and hydrogen-to-ethanol (H_2 :EtOH) ratios. Condition II (pentose liquor): (D,E) soluble phase products and (F) hydrogen-to-propionate (H_2 :HPPr) and hydrogen-to-ethanol (H_2 :EtOH) ratios. Nomenclature: HCl—citric acid, HMa—malic acid, HSu—succinic acid, HLa—lactic acid, HFo—formic acid, HAc—acetic acid (resulting from fermentation in condition I), HAc Total—total acetic acid (resulting from both bagasse hydrolysate and substrate fermentation in condition II); HAc Bio—acetic acid (resulting from fermentation in condition II), HPr—propionic acid, HBu—butyric acid, HVa—valeric acid, HCa—caproic acid, EtOH—ethanol. Note: HAc Total calculated according to Aguilar et al. [46].

The higher concentration of malate detected in experimental condition II could possibly be linked to the release of malic acid, which is part of the natural composition of plants, including sugarcane and citrus fruits. Malic acid has been previously detected in sugarcane-derived substrates, such as vinasse [73,74]. According to Figure 4D, malate presented a marked decay profile after day 10 because it could be readily metabolized by the acclimatized bacterial consortium. Malate was most likely converted to pyruvic acid, which was integrated into the ethanol fermentation reactions involving decarboxylation to acetaldehyde with a subsequent reduction in alcohol [75]. The increasing profile of ethanol production, as shown in Figure 4D, supports this hypothesis. Malate may also have been converted to lactate following malolactic fermentation [76], which has been previously suggested to occur during vinasse fermentation [77].

Caproate was another relevant soluble metabolite produced in the fermentation of pentose liquor. According to the metabolite profiles shown in Figures 3B and 4D, caproic acid production is likely related to a pathway described elsewhere [78], in which simultaneous hydrogen and caproic acid production was feasible but resulted in low amounts of biohydrogen. These authors reported that caproic acid could also be formed through the

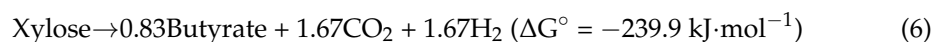
secondary fermentation of ethanol and acetate or ethanol and butyrate. Because acetate was one of the major products found in experimental condition II (Figure 4E), it is likely that acidogenic bacteria used acetate as an alternative terminal acceptor for the reducing equivalents during caproic acid synthesis [79]. Moreover, during the fermentation of pentoses, elevated production of ethanol (Figure 4D) potentially resulted from the above-mentioned metabolic pathway. This observation is consistent with the assumption that some caproate-producing bacteria formed a syntrophic relationship with ethanol-producing bacteria [80]. Another factor supporting the existence of caproate-producing bacteria in the mixed culture is the occurrence of spore-forming *Clostridium kluyveri*, which is known to be resistant to the harsh environments and treatments (e.g., highly acidic conditions) used for selecting HPB [78].

Regarding acetate production, the fermentative pathway of xylose leading to this product can occur spontaneously [27], as shown in Reaction (5). In experimental condition I, acetic acid was the major metabolite produced (Figure 4B), thus implying improved hydrogen yields due to coupled reactions in the metabolic pathway, as demonstrated by Reaction (5). However, stable or increasing hydrogen production was not observed (Figure 3A). On the contrary, the biohydrogen generation profile demonstrated a peak followed by continuous decay, which was possibly caused by the increasing dominance of homoacetogenic bacteria (Reaction 1). A marked decrease in the volumetric biogas production indicated that carbon dioxide and hydrogen were diverted to acetate production, as stoichiometrically demonstrated in Reaction (1). In experimental condition II, a mean concentration of acetate equal to $784.55 \text{ mg}\cdot\text{L}^{-1}$ (HAc Total; Figure 4E) was produced; however, a major part of this production was derived from the hydrolysis of acetyl groups bound to hemicellulosic monomers of SCB. Because the protocol described by Aguilar et al. [46] was followed in this study, the calculations pointed to the physicochemical release of $642 \text{ mg}\cdot\text{L}^{-1}$ of acetate and enabled biologically produced acetic acid to be estimated (HAc Bio; Figure 4E), which was $142.55 \text{ mg}\cdot\text{L}^{-1}$ on average. Whereas in this condition, the acetate production was unstable (HAc Bio; Figure 4E), the generation of this metabolite in condition I showed an increasing profile (Figure 4B). This result indicates the occurrence of homoacetogenic reactions in condition I and the limitations of this biochemical route in experimental condition II. The high concentration of acetate derived from pretreatment could have inhibited the homoacetogenic pathway in the reactor fed with the SCB hydrolysate (condition II) because the accumulation of non-dissociated organic acids is deleterious to acidogenic bacteria [81]. However, a systemic inhibition, i.e., affecting all fermentative groups (including HPB), should be expected in this case. Hence, although continuous, the biogas production in condition II was most likely not high enough to stimulate the development of homoacetogens.

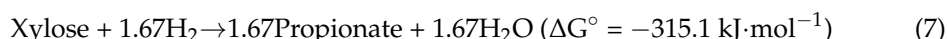


Butyrate production was detected at concentrations ranging from 60 to $100 \text{ mg}\cdot\text{L}^{-1}$ in condition I and from 133 to $361 \text{ mg}\cdot\text{L}^{-1}$ in condition II. The reasons for these differences are likely related to the increasing utilization of the substrate in condition II (Figure 3B) and the occurrence of different terminal electron acceptors in condition I, as demonstrated by the production of acetate (Figure 4B) and metabolic trends in the formation of propionate and ethanol (Figure 4C). Similar to acetate production, the generation of butyric acid occurred simultaneously with the production of hydrogen; however, the yield was lower [82], as shown in Reaction (6). In experimental condition II, the lower biohydrogen generation was possibly determined by the biochemical yield demonstrated in Reaction (6), which implied half of the biohydrogen yield compared to that obtained when acetic acid was the by-product (Reaction 5). In both experimental conditions, the predominance of acetate and butyrate as major metabolites suggested the initial occurrence of a butyrate-acetate metabolic pathway, in which *Clostridium* sp. is the specific dominant strain. The same observation was made in previous studies utilizing UAPBR systems and natural fermentation for inoculation procedures [41,42,52]. In the study by Peixoto et al. [41], 16S rRNA sequencing

analysis showed a 91% similarity to *Clostridium* sp, which comprised the butyrate producers *C. acetobutylicum*, *C. tyrobutyricum*, and *C. beijerinckii*.



The propionate concentration in condition I increased from 50 to 105 mg·L^{−1}, with a mean production of 66.3 mg·L^{−1}. In condition II, propionate was also detected at an increment of 230 mg·L^{−1}, which resulted in an increase from 112 to 342 mg·L^{−1}. Although this increase is interesting due to the market value of propionic acid [21], the generation of this metabolite in biohydrogen-producing reactors results in a lower yield. This hydrogen-consuming pathway [13,27,34] is demonstrated by Reaction (7), usually taking place when high hydrogen partial pressures are established in the reactors. One of the factors influencing the instability of biohydrogen production in condition II probably included the peaks of propionate concentration on days 12, 23, and 33 (Figure 4E). This hypothesis was valid because the hydrogen concentration had a simultaneous decrease when these propionate peaks were detected. On the other hand, the decrease in biohydrogen production in condition I could more likely be explained by its conversion into acetate in the homoacetogenic pathway because the average production of propionate was quite low (66 mg·L^{−1}) compared to that observed in experimental condition II (228 mg·L^{−1}). In spite of the elevated production of propionic acid in condition II, the H₂/Propionate ratio (Figure 4F) showed an increase in its trend because hydrogen production did not cease. On the contrary, in condition I, the H₂/Propionate ratio was close to 0 by the end of the reactor operation due to the interruption of hydrogen production despite the production of acetate (Figure 4B).



In addition to the production of hydrogen and volatile organic acids, a relatively low amount of ethanol was generated from the xylose media and SCB-derived pentose liquor. The results in Figure 4A,B show the mean ethanol productions of 43 and 110 mg·L^{−1} in conditions I and II, respectively. This decrease in the trend of the H₂/Ethanol ratio in condition I occurred due to the progressive termination of biohydrogen production (Figure 3A); however, in experimental condition II, the profile of the H₂/Ethanol ratio (Figure 4F) was different due to the opposite dynamics in biohydrogen production.

According to the mass flow rate shown in Table 2, the average missing equivalents in experimental condition I was lower than 2%, implying a 98% correspondence between the calculations and experimental data. One explanation for this unbalance could be the presence of the bacteria *Klebsiella* sp., which was previously identified in acidogenic inocula obtained from carbohydrate natural fermentation [41,83]. This microbial group was involved in the production of ethanol and 2,3-butanediol: a metabolite that was not monitored by the analytical methods used in this study. This metabolite was produced under limited oxygen and low pH conditions [84], similar to those utilized in the experiment presented herein. In experimental condition II, the sum of organic metabolites exceeded the mass balance in 207.24 mg·h^{−1}, causing an approximate lack of correspondence at 11%. In this case, it is not likely that the formation of undetected metabolites or the presence of alternative electron sinks accounted for the unbalance. Rather, the other carbon sources that were not monitored, such as glucose (1.58%), galactose (2.81%), rhamnose (6.14%), and arabinose (7.12%), were probably fermented and led to the formation of their own metabolites besides those produced with xylose (82.4%).

Table 2. Mass flowrate in experimental conditions I and II. Values in parentheses correspond to the day in which each maximum value was obtained.

Mass Flow Rate (mg·h ⁻¹)	Condition I (Xylose-Based Wastewater)		Condition II (Pentose Liquor)	
	Maximum	Mean	Maximum	Mean
Influent xylose	4171.12 (10)	2096.68 ± 811.4	2256.85 (33)	1886.92 ± 141.3
Effluent xylose	2591.34 (4)	1148.13 ± 491.2	1312.13 (2)	610.28 ± 173.7
Citric acid	72.28 (36)	70.71 ± 1.07	ND	ND
Malic acid	87.19 (17)	45.89 ± 16.8	69.31 (2)	56.82 ± 6.6
Succinic acid	47.22 (25)	46.88 ± 0.3	ND	ND
Lactic acid	119.36 (3)	107.37 ± 7.0	248.73 (4)	229.87 ± 9.1
Formic acid	28.11 (22)	24.86 ± 2.0	ND	ND
Acetic acid	305.76 (36)	150.66 ± 61.2	379.20 ¹ (10)	186.72 ¹ ± 89.8
Propionic acid	125.92 (31)	79.63 ± 17.0	447.80 (33)	298.52 ± 78.6
Isobutyric acid	94.07 (3)	72.33 ± 8.7	156.48 (26)	119.34 ± 28.0
n-Butyric acid	120.80 (8)	85.53 ± 15.2	473.39 (18)	299.23 ± 71.1
Isovaleric acid	140.55 (10)	109.02 ± 22.4	88.20 (18)	53.24 ± 18.8
n-Valeric acid	72.65 (36)	69.61 ± 1.6	85.62 (31)	64.43 ± 13.3
Caproic acid	ND	ND	32.40 (18)	17.47 ± 4.0
Ethanol	72.05 (29)	51.46 ± 11.0	215.66 (26)	144.47 ± 22.5
Hydrogen	11.24 (8)	1.84 ± 0.003	2.70 (16)	0.55 ± 0.0008
Carbon dioxide	82.43 (8)	15.70 ± 0.02	68.04 (16)	13.22 ± 0.02
Sum (soluble + gas metabolites)	NC	2079.62	NC	2094.16
Correspondence (%) ²	NC	99.2	NC	111.0

¹ Resulting from substrate fermentation. ² Corresponds to the ratio between the sum of metabolites and the influent xylose. Legend: ND—not detected, NC—not calculated (the sum of metabolites and their correspondence were not calculated for maximum values because they were observed in different days).

According to Table 3, the production of the main volatile organic acids was comparable to other studies reported in the literature, while H₂ production was significantly lower. In the studies by Wu et al. [36] and Lin et al. [34], 20 g·L⁻¹ of xylose was used as the initial substrate concentration, which was more than ten-fold higher than the sugar concentrations used to feed the packed-bed reactor in this study. The effect of the temperature should also be considered because other studies with an equivalent substrate concentration reported hydrogen yields higher than those obtained in this study [26,32,34,36]. Lin et al. [34] demonstrated that increasing temperatures (from 30 to 50 °C) promoted higher hydrogen yields and production rates. In their study, temperatures of 30, 35, 40, 45, and 50 °C corresponded to 0.4, 0.5, 0.3, 0.8, and 1.3 mol H₂·mol⁻¹xylose, respectively. Thus, it is likely that the low biohydrogen production in the UAPBR was greatly influenced by the initial substrate's concentration (or applied OLR, as discussed in Section 3.1) and operation temperature. However, the production of both butyric and propionic acids (Table 3) in the UAPBR was greater than that reported by Wu et al. [36] and Patra et al. [26].

3.3. Preliminary Analysis of Biohydrogen, VOA and Cogeneration Potential in a Pentose Liquor-Based Biorefinery

The experimental results provided the main parameters with which to develop and analyze a biorefinery performance in four independent scenarios, as detailed in Section 2.5 and depicted in Figure 5. According to Table 4, a comparison between Scenarios 1 and 2 suggested that exclusively producing 1G and 2G of ethanol (Scenario 2) was more profitable than using 50% of SCB for cogeneration and 50% for 2G ethanol production (Scenario 1) due to fuel [85] and electricity prices [86]. In the abovementioned cases, the economic potential per day of a sugarcane mill operation was 19.6% (Scenario 2) and 26.4% (Scenario 1), which is lower than that reported in Scenario 3. Null environmentally friendly potential was found in Scenarios 1 and 2 because pentose liquor derived from the SCB pretreatment was

not used as a raw material for biohydrogen, VOA, or methane production and could result in the accumulation of 16,800 and 33,600 m³·d^{−1} of 2G ethanol byproducts, respectively. In Scenario 3, the greatest economic potential was achieved because the extraction of value-added VOA was considered. Among these acids, acetate is used as a precursor to industrial polymers, including mainly the vinyl acetate monomer [87], butyrate is used in industrial thermoplastics in the form of cellulose acetate butyrate [23], propionate is utilized as a food preservative [88], and lactate is involved in the production of biodegradable polymers, also known as polylactides [24]. In addition, the separation of these organic acids might have a low cost if performed by an ion exchange resin, as demonstrated elsewhere [16]. In terms of energy production, Scenario 4 provided relevant energetic potential; however, organic acids could not be directly recovered. Rather, they were considered substrates for methane production [89]. In this scenario, methane was considered the raw material for on-site cogeneration because this application did not require purification and also allowed local carbon offset projects with a cogeneration price (64.70 USD·MWh^{−1}) that is more attractive than a commodity price of 2.77 USD per 10³ ft³ [90]. If the energetic potential depended on burning hydrogen alone, the maximum energy production would be 0.73 MWh, which is not significant for achieving profitability (Scenarios 3 and 4). However, hydrogen must be considered as an available surplus of this process because its production is obligatorily coupled to that of VOA (Reactions 5–6). An on-site application for biohydrogen could be the complete fueling of 56 hydrogen fuel cell vehicles per day with driving ranges of 240 miles [91], which is sufficient for the plant's complete fleet of cars. According to Table 4, the major advantage of Scenarios 3 and 4 is that in the production of organic acids or methane, the environmental impact (assessed as the COD reduction) of the 2G ethanol byproducts could be reduced by 62.7% through the separation/extraction of organic acids (acetate, butyrate, propionate, and lactate) or approximately 75% when employing a process based on sequential hydrogen and methane production [92]. Specifically in Scenario 3, organic matter removal could be further increased through the methanization of the VOA that were not extracted as raw materials for the chemical industry, namely the citric, malic, succinic, formic, valeric, and caproic acids.

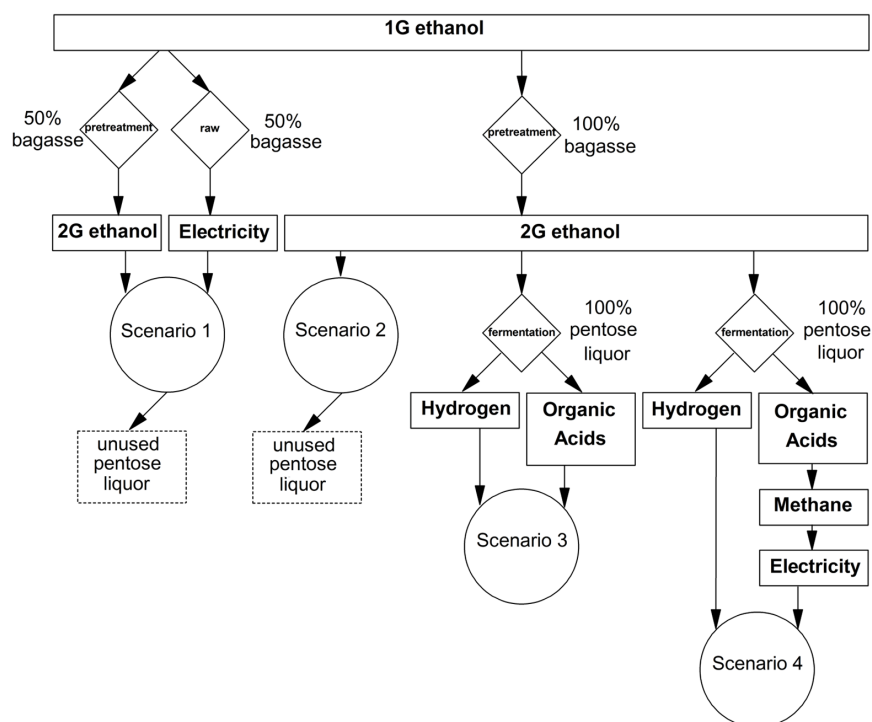


Figure 5. Second-generation sugarcane biorefinery schemes including potential biotechnological uses for pentose liquor.

Table 3. Comparative analysis of systems used for biohydrogen and organic acids production from pentoses.

Reactor	Xylose Concentration (gCOD·L ⁻¹)	Temp.	pH	HY	VHPR	VOA Production (mg·h ⁻¹)			Reference
						HBu	HPr	HAc	
CSTR	20.0	50	6.5	0.4	6600	264	1767	1601	[36]
AGSB	20.0	40	6.5	0.6	19,680	835	173	820	[36]
Batch ²	1.5	37	5.5	1.5	-	853 ¹	4.53 ¹	149 ¹	[26]
UAPBR	1.7	25	6.7	0.08	398.4	120.8	125.9	305.76	This study
UAPBR ²	1.7	25	5.9	0.04	120	473.4	447.8	379.20	This study

¹ Terminal soluble metabolite concentrations (measured at the end of the experimental runs). ² Using pentose liquor. Nomenclature: Temp.—temperature (°C), HY—hydrogen yield (mol H₂·mol⁻¹xylose), VHPR—volumetric hydrogen production rate (mL H₂·L⁻¹·d⁻¹), VOA—volatile organic acids, HBu—butyric acid, HPr—propionic acid, HAc—acetic acid, CSTR—continuous stirred-tank reactor, AGBS—activated carbon-assisted agitated granular sludge bed, UAPBR—upflow anaerobic packed-bed reactor.

Table 4. Energetic, economic and environmental aspects for different second-generation sugarcane biorefinery schemes.

Scenarios/Products		1	2	3	4
		1G Ethanol 50%—2G Ethanol 50%—Cogeneration	1G Ethanol 2G Ethanol	1G Ethanol 2G Ethanol Hydrogen Organic Acids	1G Ethanol 2G Ethanol Hydrogen Methane
1G Ethanol	Production (m ³ ·d ⁻¹) ¹	987.60	987.60	987.60	987.60
	Econ. Pot. (USD·d ⁻¹) ²	521,924.96	521,924.96	521,924.96	521,924.96
2G Ethanol	Production (m ³ ·d ⁻¹) ³	149.69	299.37	299.37	299.37
	Econ. Pot. (USD·d ⁻¹) ²	79,106.83	158,213.66	158,213.66	158,213.66
Hydrogen	Production (m ³ ·d ⁻¹) ⁴	NA	NA	19.06	19.06
	Econ. Pot. (USD·d ⁻¹) ⁵	NA	NA	2897.44	2897.44
Organic Acids (HLA, HAc, HPr, HBu)	Production (kg·d ⁻¹) ⁶	NA	NA	201,144.05	NA
	Econ. Pot. (USD·d ⁻¹) ⁷	NA	NA	162,693.67	NA
Energy (cogeneration ⁸ /methane ^{11,12})	Production (m ³ ·d ⁻¹)	NA	NA	NA	118,931.60 ¹¹
	Energ. Pot. (MWh)	334.32 ⁸	NA	NA	806.73 ¹²
	Econ. Pot. (USD·d ⁻¹)	23,422.82 ⁹	NA	NA	52,192.02 ⁹
Total Energetic potential (MWh)		334.32	NA	NA	806.73
Total Economic potential (USD·d ⁻¹)		622,660.68	680,138.61	845,729.72	735,228.08
Total Environmental potential (COD removal percentage)		NA	NA	62.7 ¹⁰	74.7 ¹¹

¹ Medium-sized sugarcane distillery (milling capacity = 500 ton·h⁻¹) considering 1G ethanol yield [93].

² According to the anhydrous ethanol market price provided by the Center for Advanced Studies on Applied Economics (CEPEA/ESALQ/USP) [85]. ³ Considering the 2G ethanol yield obtained exclusively from the cellulosic fraction [94]. ⁴ According to the mean hydrogen yield obtained in experimental condition II. ⁵ According to the hydrogen market price reported by the U.S. Department of Energy [95]. ⁶ According to the mean organic acid yield obtained in experimental condition II. ⁷ According to HLA, HAc, HPr, and HBu reference prices [96]. ⁸ Calculated as the surplus electricity of a distillery producing only 1G ethanol [93]. ⁹ According to the market price defined by alternative energy auctions, as released by the Brazilian Energy Research Office (EPE/MME) [86]. ¹⁰ Calculated as the COD of all organic matter minus the COD of the extracted acids (HLA, HAc, HPr, HBu). ¹¹ Considering 350 mL CH₄·g⁻¹COD removed [89] and 74.7% methanization efficiency of vinasse [92]. ¹² Considering CH₄ properties [85] and combined cycle turbines [97]. Nomenclature: 1G—first generation, 2G—second generation, HAc—acetic acid, HBu—butyric acid, HLA—lactic acid, HPr—propionic acid, NA—not applicable.

4. Conclusions

Biohydrogen and volatile organic acids were produced using both a xylose-based media and sugarcane bagasse-derived pentose liquor. The fermentation of the pretreatment-derived pentose liquor generated a 25% higher volatile organic acid concentration compared to that obtained with the xylose-based media. The differences in the composition of both substrates triggered different fermentative metabolic pathways, leading to the stimulus of homoacetogenesis when using xylose and to the occurrence of biohydrogen

production coupled to acetate and butyrate buildup when using pentose liquor. Overall, higher biohydrogen production rates could be observed when modifying the operating conditions applied in the packed-bed reactor, such as applying high organic loading rates and increasing the temperature to achieve thermophilic conditions. Nevertheless, the continuous operation of the reactor yielded both operational and performance parameters that enabled the simulation of the application of dark fermentation in a medium-sized distillery. The best estimate indicated that recovering hydrogen and organic acids from pentose liquor had the potential to enhance profits in an ethanol production plant (1G and 2G) by 24.3% with a simultaneous environmental impact reduction of 62.7%. Therefore, developing the present fermentation technology seems to be crucial for improving the sustainability of conventional 1G and 2G sugarcane biorefineries.

Author Contributions: Conceptualization, D.M.F.L.; methodology, M.A.d.L.; formal analysis, F.V.F.; investigation, W.K.M.; resources, M.A.d.L.; writing—original draft preparation, G.P. and G.M.; writing—review and editing, L.T.F.; visualization, I.P.; supervision, M.Z.; project administration, M.Z.; funding acquisition, M.Z. All authors have read and agreed to the published version of the manuscript.

Funding: This research was funded by the FUNDAÇÃO DE AMPARO À PESQUISA DO ESTADO DE SÃO PAULO, grant numbers 2008/56255-9, 2009/17539-4 and 2009/15984-0. The APC was waived by the journal.

Data Availability Statement: The data presented in this study are available on request from the corresponding author.

Conflicts of Interest: The authors declare no conflict of interest.

References

1. Lago, A.C.; Bonomi, A.; Cavalett, O.; Cunha, M.P.; Lima, M.A. Sugarcane as a carbon source: The Brazilian case. *Biomass Bioenergy* **2012**, *46*, 5–12. [CrossRef]
2. Poggi-Varaldo, H.M.; Munoz-Paez, K.M.; Escamilla-Alvarado, C.; Robledo-Narváez, P.N.; Ponce-Noyola, M.T.; Calva-Calva, G.; Ríos-Leal, E.; Galíndez-Mayer, J.; Estrada-Vázquez, C.; Ortega-Clemente, A.; et al. Biohydrogen, biomethane and bioelectricity as crucial components of biorefinery of organic wastes: A review. *Waste Manag. Res.* **2014**, *32*, 353–365. [CrossRef] [PubMed]
3. Moraes, E.R.; Junqueira, T.L.; Sampaio, I.L.M.; Dias, M.O.S.; Rezende, M.C.A.F.; Jesus, C.D.F.; Klein, B.C.; Gómez, E.O.; Mantelatto, P.E.; Maciel Filho, R.; et al. Biorefinery alternatives. In *Virtual biorefinery: An Optimization Strategy for Renewable Carbon Valorization*; Bonomi, A., Cavalett, O., Cunha, M.P., Lima, M.A.P., Eds.; Springer: London, UK, 2016; pp. 53–132.
4. Dias, M.O.S.; Junqueira, T.L.; Sampaio, I.L.M.; Chagas, M.F.; Watanabe, M.D.B.; Moraes, E.R.; Gouveia, V.L.R.; Klein, B.C.; Rezende, M.C.A.F.; Cardoso, T.F.; et al. Use of the VSB to assess biorefinery strategies. In *Virtual biorefinery: An Optimization Strategy for Renewable Carbon Valorization*; Bonomi, A., Cavalett, O., Cunha, M.P., Lima, M.A.P., Eds.; Springer: London, UK, 2016; pp. 189–256.
5. Rabelo, S.C.; Carrere, H.; Maciel Filho, R.; Costa, A.C. Production of bioethanol, methane and heat from sugarcane bagasse in a biorefinery concept. *Bioresour. Technol.* **2011**, *102*, 7887–7895. [CrossRef] [PubMed]
6. CONAB. Acompanhamento da Safra Brasileira de Cana-de-Açúcar; Safra 2023/24—Primeiro Levantamento; CONAB: Brasília, Brasil, 2023. Available online: https://www.conab.gov.br/info-agro/safras/cana/boletim-da-safra-de-cana-de-acucar/item/download/47193_22dfa86f63aa61cd8e405419b30d9262 (accessed on 27 June 2023). (In Portuguese)
7. Dias, M.O.S.; Junqueira, T.L.; Cavalett, O.; Pavanetto, L.G.; Cunha, M.P.; Jesus, C.D.F.; Maciel Filho, R.; Bonomi, A. Biorefineries for the production of first and second generation ethanol and electricity from sugarcane. *Appl. Energy* **2013**, *109*, 72–78. [CrossRef]
8. Dias, M.O.S.; Junqueira, T.L.; Rossel, C.E.; Maciel Filho, R.; Bonomi, A. Evaluation of process configurations for second generation integrated with first generation bioethanol production from sugarcane. *Fuel Process. Technol.* **2013**, *109*, 84–89. [CrossRef]
9. Zhou, M.; Lü, X. Strategies on simultaneous fermentation of pentose and hexose to bioethanol. In *Advances in 2nd Generation of Bioethanol Production*; Lü, X., Ed.; Woodhead Publishing: Duxford, UK, 2021; pp. 161–211.
10. Sriariyanun, M.; Gundupalli, M.P.; Phakeenuya, V.; Phusantisampan, T.; Cheng, Y.S.; Venkatachalam, P. Biorefinery Approaches For Production Of Cellulosic Ethanol Fuel Using Recombinant Engineered Microorganisms. *J. Appl. Sci. Eng.* **2023**, *27*, 1985–2005.
11. Ghimire, A.; Frunzo, L.; Pirozzi, F.; Trably, E.; Escudie, R.; Lens, P.N.L.; Esposito, G. A review on dark fermentative biohydrogen production from organic biomass: Process parameters and use of by-products. *Appl. Energy* **2015**, *144*, 73–95. [CrossRef]
12. Elbeshbishy, E.; Dhar, B.R.; Nakhla, G.; Lee, H.S. A critical review on inhibition of dark biohydrogen fermentation. *Renew. Sustain. Energy Rev.* **2017**, *79*, 656–668. [CrossRef]
13. Hawkes, F.R.; Dinsdale, R.; Hawkes, D.L.; Hussy, I. Sustainable fermentative hydrogen production: Challenges for process optimization. *Int. J. Hydrogen Energy* **2002**, *27*, 1339–1347. [CrossRef]

14. Show, K.Y.; Lee, D.J.; Tay, J.H.; Lin, C.Y.; Chang, J.S. Biohydrogen production: Current perspectives and the way forward. *Int. J. Hydrogen Energy* **2012**, *37*, 15616–15631. [\[CrossRef\]](#)
15. Das, D.; Veziroglu, T. Hydrogen production by biological processes: A survey of literature. *Int. J. Hydrogen Energy* **2001**, *26*, 13–28. [\[CrossRef\]](#)
16. Leite, J.A.C.; Fenandes, B.S.; Pozzi, E.; Barboza, M.; Zaiat, M. Application of an anaerobic packed-bed biobioreactor for the production of hydrogen and organic acids. *Int. J. Hydrogen Energy* **2008**, *33*, 579–586. [\[CrossRef\]](#)
17. Ramos, L.R.; Silva, E.L. Thermophilic hydrogen and methane production from sugarcane stillage in two-stage anaerobic fluidized bed reactors. *Int. J. Hydrogen Energy* **2020**, *45*, 5239–5251. [\[CrossRef\]](#)
18. Ferreira, T.B.; Rego, G.C.; Ramos, L.R.; Menezes, C.A.; Silva, E.L. Improved dark fermentation of cane molasses in mesophilic and thermophilic anaerobic fluidized bed reactors by selecting operational conditions. *Int. J. Energy Res.* **2020**, *44*, 10442–10452. [\[CrossRef\]](#)
19. Fuess, L.T.; Braga, A.F.M.; Eng, F.; Gregoracci, G.; Saia, F.T.; Zaiat, M.; Lens, P.N.L. Solving the bottlenecks of sugarcane vinasse biodigestion: Impacts of temperature and substrate exchange on sulfate removal during dark fermentation. *Chem. Eng. J.* **2023**, *455*, 140965. [\[CrossRef\]](#)
20. Menezes, C.A.; Almeida, P.S.; Delforno, T.P.; Oliveira, V.M.; Sakamoto, I.K.; Varesche, M.B.A.; Silva, E.L. Relating biomass composition and the distribution of metabolic functions in the co-fermentation of sugarcane vinasse and glycerol. *Int. J. Hydrogen Energy* **2023**, *48*, 8837–8853. [\[CrossRef\]](#)
21. Kim, H.; Jeon, B.S.; Sang, B.I. An efficient new process for the selective production of odd-chain carboxylic acids by simple carbon elongation using *Megasphaera hexanoica*. *Sci. Rep.* **2019**, *9*, 11999. [\[CrossRef\]](#)
22. Bastidas-Oyanedel, J.R.; Schmidt, J.E. Increasing profits in food waste biorefinery—A techno-economic analysis. *Energies* **2018**, *11*, 1551. [\[CrossRef\]](#)
23. Brady, G.S.; Clauser, H.R.; Vaccari, J.A. *Materials Handbook*, 15th ed.; McGraw-Hill Professional: New York, NY, USA, 2002.
24. Napoothiri, K.M.; Nair, N.R.; John, R.P. An overview of the recent developments in polylactide (PLA) research. *Bioresour Technol.* **2010**, *101*, 6493–8501.
25. Oliveira, G.H.D.; Niz, M.Y.K.; Zaiat, M.; Rodrigues, J.A.D. Effects of organic loading rate on polyhydroxyalkanoate production from sugarcane stillage by mixed microbial cultures. *Appl. Biochem. Biotechnol.* **2019**, *189*, 1039–1055. [\[CrossRef\]](#)
26. Pattr, S.; Sangyoka, S.; Boonmee, M.; Reungsang, A. Bio-hydrogen Production from the Fermentation of Sugarcane Bagasse Hydrolysate by *Clostridium butyricum*. *Int. J. Hydrogen Energy* **2008**, *33*, 5256–5265. [\[CrossRef\]](#)
27. Kongjan, P.; Min, B.; Angelidaki, I. Biohydrogen production from xylose at extreme thermophilic temperatures (70 °C) by mixed culture fermentation. *Water Res.* **2009**, *43*, 1414–1424. [\[CrossRef\]](#) [\[PubMed\]](#)
28. Baêta, B.E.L.; Lima, D.R.S.; Balena Filho, J.G.; Adarme, O.F.H.; Gurgel, L.V.A.; Aquino, S.F. Evaluation of hydrogen and methane production from sugarcane bagasse hemicellulose hydrolysates by two-stage anaerobic digestion process. *Bioresour Technol.* **2016**, *218*, 436–446. [\[CrossRef\]](#) [\[PubMed\]](#)
29. Thungklin, P.; Sittijunda, S.; Reungsang, A. Sequential fermentation of hydrogen and methane from steam-exploded sugarcane bagasse hydrolysate. *Int. J. Hydrogen Energy* **2018**, *43*, 9924–9934. [\[CrossRef\]](#)
30. Chatterjee, S.; Mohan, S.V. Simultaneous production of green hydrogen and bioethanol from segregated sugarcane bagasse hydrolysate streams with circular biorefinery design. *Chem. Eng. J.* **2021**, *425*, 130386. [\[CrossRef\]](#)
31. Fangkum, A.; Reungsang, A. Biohydrogen production from mixed xylose/arabinose at thermophilic temperature by anaerobic mixed cultures in elephant dung. *Int. J. Hydrogen Energy* **2011**, *36*, 13928–13938. [\[CrossRef\]](#)
32. Maintinguer, S.I.; Fernandes, B.S.; Duarte, I.C.S.; Saavedra, N.K.; Adorno, M.A.T.; Varesche, M.B.A. Fermentative hydrogen production with xylose by *Clostridium* and *Klebsiella* species in anaerobic batch bioreactors. *Int. J. Hydrogen Energy* **2011**, *36*, 13508–13517. [\[CrossRef\]](#)
33. Lin, C.; Cheng, C. Fermentative hydrogen production from xylose using anaerobic mixed microflora. *Int. J. Hydrogen Energy* **2006**, *31*, 832–840. [\[CrossRef\]](#)
34. Lin, C.; Wu, C.; Hung, C. Temperature effects on fermentative hydrogen production from xylose using mixed anaerobic cultures. *Int. J. Hydrogen Energy* **2008**, *33*, 43–50. [\[CrossRef\]](#)
35. Zhao, C.; Karakashev, D.; Lu, W.; Wang, H.; Angelidaki, I. Xylose fermentation to biofuels (hydrogen and ethanol) by extreme thermophilic (70 °C) mixed culture. *Int. J. Hydrogen Energy* **2010**, *5*, 3415–3422. [\[CrossRef\]](#)
36. Wu, S.Y.; Lin, C.Y.; Lee, K.S.; Hung, C.H.; Chang, J.S.; Lin, P.J.; Chang, F.Y. Dark Fermentative Hydrogen Production from Xylose in Different Bioreactors Using Sewage Sludge Microflora. *Energy Fuels* **2008**, *22*, 113–119. [\[CrossRef\]](#)
37. Dessi, P.; Lakaniemi, A.M.; Lens, P.N.L. Biohydrogen production from xylose by fresh and digested activated sludge at 37, 55 and 70 °C. *Water Res.* **2017**, *115*, 120–129. [\[CrossRef\]](#)
38. Baik, J.H.; Jung, J.H.; Sim, Y.B.; Park, J.H.; Kim, S.M.; Yang, J.; Kim, S.H. High-rate biohydrogen production from xylose using a dynamic membrane bioreactor. *Bioresour. Technol.* **2022**, *344*, 126205. [\[CrossRef\]](#)
39. Silva, V.; Rabelo, C.A.B.S.; Camargo, F.P.; Sakamoto, I.K.; Silva, E.L.; Varesche, M.B.A. Optimization of Key Factors Affecting Hydrogen and Ethanol Production from Xylose by *Thermoanaerobacterium calidifontis* VCS1 Isolated from Vinasse Treatment Sludge. *Waste Biomass Valorization* **2022**, *13*, 1897–1912. [\[CrossRef\]](#)
40. Lima, D.M.F.; Zaiat, M. The influence of the degree of back-mixing on hydrogen production in an anaerobic fixed-bed reactor. *Int. J. Hydrogen Energy* **2012**, *37*, 9630–9635. [\[CrossRef\]](#)

41. Peixoto, G.; Saavedra, N.K.; Varesche, M.B.A.; Zaiat, M. Hydrogen production from soft-drink wastewater in an upflow anaerobic packed-bed bioreactor. *Int. J. Hydrogen Energy* **2011**, *36*, 8953–8966. [\[CrossRef\]](#)
42. Penteado, E.D.; Lazaro, C.Z.; Sakamoto, I.K.; Zaiat, M. Influence of seed sludge and pretreatment method on hydrogen production in packed-bed anaerobic reactors. *Int. J. Hydrogen Energy* **2013**, *38*, 6137–6145. [\[CrossRef\]](#)
43. Ferraz Jr, A.D.N.; Etchebehere, C.; Zaiat, M. High organic loading rate on thermophilic hydrogen production and metagenomic study at an anaerobic packed-bed reactor treating a residual liquid stream of a Brazilian biorefinery. *Bioresour. Technol.* **2015**, *186*, 81–88. [\[CrossRef\]](#)
44. Fuess, L.T.; Kiyuna, L.S.M.; Garcia, M.L.; Zaiat, M. Operational strategies for long-term biohydrogen production from sugarcane stillage in continuous acidogenic packed-bed reactor. *Int. J. Hydrogen Energy* **2016**, *41*, 8132–8145. [\[CrossRef\]](#)
45. Corbari, S.D.M.L.; Andreani, C.L.; Torres, D.G.B.; Eng, F.; Gomes, S.D. Strategies to improve the biohydrogen production from cassava wastewater in fixed-bed reactors. *Int. J. Hydrogen Energy* **2019**, *44*, 17214–17223. [\[CrossRef\]](#)
46. Aguilar, R.; Ramirez, J.A.; Garrote, G.; Vazquez, M. Kinetic study of the acid hydrolysis of sugarcane bagasse. *J. Food Eng.* **2002**, *55*, 309–318. [\[CrossRef\]](#)
47. APHA; AWWA; WEF. *Standard Methods for the Examination of Water and Wastewater*, 22nd ed.; APHA: Washington, DC, USA, 2012.
48. Dubois, M.; Gilles, K.A.; Hamilton, J.K.; Rebers, P.A.; Smith, F. Colorimetric methods for determination of sugar and related substance. *Anal. Chem.* **1956**, *28*, 350–356. [\[CrossRef\]](#)
49. Mockaitis, G.; Rodrigues, J.A.D.; Foresi, E.; Zaiat, M. Toxic effects of cadmium (Cd²⁺) on anaerobic biomass: Kinetic and metabolic implications. *J. Environ. Manag.* **2012**, *106*, 75–84. [\[CrossRef\]](#) [\[PubMed\]](#)
50. Perna, V.; Castelló, E.; Wenzel, J.; Zampol, C.; Lima, D.M.F.; Borzacconi, L.; Varesche, M.B.; Zaiat, M.; Etchebehere, C. Hydrogen production in an upflow anaerobic packed bed reactor used to treat cheese whey. *Int. J. Hydrogen Energy* **2013**, *38*, 54–62. [\[CrossRef\]](#)
51. Ferraz, A.D.N., Jr.; Etchebehere, C.; Zaiat, M. Mesophilic hydrogen production in acidogenic packed-bed reactors (APBR) using raw sugarcane vinasse as substrate: Influence of support materials. *Anaerobe* **2015**, *34*, 94–105.
52. Lima, D.M.F.; Moreira, W.K.; Zaiat, M. Comparison of the use of sucrose and glucose as a substrate for hydrogen production in an upflow anaerobic fixed-bed reactor. *Int. J. Hydrogen Energy* **2013**, *38*, 15074–15083. [\[CrossRef\]](#)
53. Anzola-Rojas, M.P.; Fonseca, S.G.; Silva, C.C.; Oliveira, V.M.; Zaiat, M. The use of the carbon/nitrogen ratio and specific organic loading rate as tools for improving biohydrogen production in fixed-bed reactors. *Biotechnol. Rep.* **2015**, *5*, 46–54. [\[CrossRef\]](#)
54. Saady, N.M.C. Homoacetogenesis during hydrogen production by mixed cultures dark fermentation. *Int. J. Hydrogen Energy* **2013**, *38*, 13172–13191. [\[CrossRef\]](#)
55. Ferreira, T.B.; Rego, G.C.; Ramos, L.R.; Menezes, C.A.; Soares, L.A.; Sakamoto, I.K.; Varesche, M.B.A.; Silva, E.L. HRT control as a strategy to enhance continuous hydrogen production from sugarcane juice under mesophilic and thermophilic conditions in AFBRs. *Int. J. Hydrogen Energy* **2019**, *44*, 19719–19729. [\[CrossRef\]](#)
56. Menezes, C.A.; Silva, E.L. Hydrogen production from sugarcane juice in expanded granular sludge bed reactors under mesophilic conditions: The role of homoacetogenesis and lactic acid production. *Ind. Crop. Prod.* **2019**, *138*, 111586. [\[CrossRef\]](#)
57. Freitas, I.B.F.; Menezes, C.A.; Silva, E.L. An alternative for value aggregation to the sugarcane chain: Biohydrogen and volatile fatty acids production from sugarcane molasses in mesophilic expanded granular sludge bed reactors. *Fuel* **2020**, *260*, 116419. [\[CrossRef\]](#)
58. Bernal, A.P.; Menezes, C.A.; Silva, E.L. A new side-looking at the dark fermentation of sugarcane vinasse: Improving the carboxylates production in mesophilic EGSB by selection of the hydraulic retention time and substrate concentration. *Int. J. Hydrogen Energy* **2021**, *46*, 12758–12770. [\[CrossRef\]](#)
59. Niz, M.Y.K.; Etchelet, I.; Fuentes, L.; Etchebehere, C.; Zaiat, M. Extreme thermophilic condition: An alternative for long-term biohydrogen production from sugarcane vinasse. *Int. J. Hydrogen Energy* **2019**, *44*, 22876–22887. [\[CrossRef\]](#)
60. Piffer, M.A.; Oliveira, C.A.; Bovio-Winkler, P.; Eng, F.; Etchebehere, C.; Zaiat, M.; Nascimento, C.A.O.; Fuess, L.T. Sulfate- and pH-driven metabolic flexibility in sugarcane vinasse dark fermentation stimulates biohydrogen evolution, sulfidogenesis or homoacetogenesis. *Int. J. Hydrogen Energy* **2022**, *47*, 31202–31222. [\[CrossRef\]](#)
61. Singh, A.; Müller, B.; Fuxelius, H.H.; Schnürer, A. AcetoBase: A functional gene repository and database for formyltetrahydrofolate synthetase sequences. *Database* **2019**, *2019*, baz142. [\[CrossRef\]](#)
62. Klemp, R.; Cypionka, H.; Widdel, F.; Pfennig, N. Growth with hydrogen, and further physiological characteristics of *Desulfotomaculum* species. *Arch. Microbiol.* **1985**, *143*, 203–208. [\[CrossRef\]](#)
63. Okamoto, M.; Miyahara, T.; Mizuno, O.; Noike, T. Biological hydrogen potential of materials characteristic of the organic fraction of municipal solid wastes. *Water Sci. Technol.* **2000**, *41*, 25–32. [\[CrossRef\]](#)
64. Garay-Arroyo, A.; Covarrubias, A.A.; Clark, I.; Niño, I.; Gosset, G.; Martínez, A. Response to different environmental stress conditions of industrial and laboratory *Saccharomyces cerevisiae* strains. *Appl. Microbiol. Biotechnol.* **2004**, *63*, 734–741. [\[CrossRef\]](#)
65. Ferraz, A.D.N., Jr.; Wenzel, J.; Etchebehere, C.; Zaiat, M. Effect of organic loading rate on hydrogen production from sugarcane vinasse in thermophilic acidogenic packed bed reactors. *Int. J. Hydrogen Energy* **2014**, *39*, 16852–16862.
66. Fuess, L.T.; Zaiat, M.; Nascimento, C.A.O. Novel insights on the versatility of biohydrogen production from sugarcane vinasse via thermophilic dark fermentation: Impacts of pH-driven operating strategies on acidogenesis metabolite profiles. *Bioresour. Technol.* **2019**, *286*, 121379. [\[CrossRef\]](#)

67. Rogeri, R.C.; Fuess, L.T.; Eng, F.; Borges, A.V.; Araujo, M.A.; Damianovic, M.H.R.Z.; Silva, A.J. Strategies to control pH in the dark fermentation of sugarcane vinasse: Impacts on sulfate reduction, biohydrogen production and metabolite distribution. *J. Environ. Manag.* **2023**, *325*, 116495. [CrossRef] [PubMed]
68. Fuess, L.T.; Zaiat, M.; Nascimento, C.A.O. Molasses vs. juice: Maximizing biohydrogen production in sugarcane biorefineries to diversify renewable energy generation. *J. Water Process Eng.* **2020**, *37*, 101534. [CrossRef]
69. Fuess, L.T.; Fuentes, L.; Bovio-Winkler, P.; Eng, F.; Etchebehere, C.; Zaiat, M.; Nascimento, C.A.O. Full details on continuous biohydrogen production from sugarcane molasses are unraveled: Performance optimization, self-regulation, metabolic correlations and quanti-qualitative biomass characterization. *Chem. Eng. J.* **2021**, *414*, 128934. [CrossRef]
70. Jo, J.H.; Lee, D.S.; Park, D.; Park, J.M. Biological hydrogen production by immobilized cells of *Clostridium tyrobutyricum* JM1 isolated from a food waste treatment process. *Bioresour. Technol.* **2008**, *99*, 6666–6672. [CrossRef]
71. Piffer, M.A.; Zaiat, M.; Nascimento, C.A.O.; Fuess, L.T. Dynamics of sulfate reduction in the thermophilic dark fermentation of sugarcane vinasse: A biohydrogen-independent approach targeting enhanced bioenergy production. *J. Environ. Chem. Eng.* **2021**, *9*, 105956. [CrossRef]
72. Oliveira, C.A.; Fuess, L.T.; Soares, L.A.; Damianovic, M.H.R.Z. Thermophilic biohydrogen production from sugarcane molasses under low pH: Metabolic and microbial aspects. *Int. J. Hydrogen Energy* **2020**, *45*, 4182–4192. [CrossRef]
73. Ramos, L.R.; Silva, E.L. Continuous hydrogen production from agricultural wastewaters at thermophilic and hyperthermophilic temperatures. *Appl. Biochem. Biotechnol.* **2017**, *182*, 846–869. [CrossRef]
74. Fuess, L.T.; Garcia, M.L.; Zaiat, M. Seasonal characterization of sugarcane vinasse: Assessing environmental impacts from fertirrigation and the bioenergy recovery potential through biodigestion. *Sci. Total Environ.* **2018**, *634*, 29–40. [CrossRef]
75. Lepe, J.A.S.; Leal, B.I. *Microbiología Enológica: Fundamentos de Vinificación*, 3rd ed.; Ediciones Mundi-Prensa: Madrid, Spain, 2004. (In Spanish)
76. Kolb, S.; Otte, H.; Nagel, B.; Schink, B. Energy conservation in malolactic fermentation by *Lactobacillus plantarum* and *Lactobacillus sake*. *Arch. Microbiol.* **1992**, *157*, 457–463. [CrossRef]
77. Fuess, L.T.; Santos, G.M.; Delforno, T.P.; Moraes, B.S.; Silva, A.J. Biochemical butyrate production via dark fermentation as an energetically efficient alternative management approach for vinasse in sugarcane biorefineries. *Renew. Energy* **2020**, *158*, 3–12. [CrossRef]
78. Ding, H.B.; Amy, T.G.; Wang, J.Y. Caproate formation in mixed-culture fermentative hydrogen production. *Bioresour. Technol.* **2010**, *101*, 9550–9559. [CrossRef]
79. Cavalcante, W.A.; Leitão, R.C.; Gehring, T.A.; Angenent, L.T.; Santaella, S.T. Anaerobic fermentation for n-caproic acid production: A review. *Process Biochem.* **2017**, *54*, 106–119. [CrossRef]
80. Chen, W.M.; Tseng, Z.J.; Lee, K.S.; Chang, J.S. Fermentative hydrogen production with *Clostridium butyricum* CGS5 isolated from anaerobic sewage sludge. *Int. J. Hydrogen Energy* **2005**, *30*, 1063–1070. [CrossRef]
81. Infantes, D.; González del Campo, A.; Villaseñor, J.; Fernández, F.J. Influence of pH, temperature and volatile fatty acids on hydrogen production by acidogenic fermentation. *Int. J. Hydrogen Energy* **2011**, *36*, 15595–15601. [CrossRef]
82. Thauer, R.K.; Jungermann, K.; Decker, K. Energy conservation in chemotrophic anaerobic bacteria. *Bacteriol. Rev.* **1977**, *41*, 100–180. [CrossRef]
83. Fernandes, B.S.; Peixoto, G.; Albrecht, F.R.; Del Aguila, N.K.S.; Zaiat, M. Potential to produce biohydrogen from various wastewaters. *Energy Sustain. Dev.* **2010**, *14*, 143–148. [CrossRef]
84. Wu, K.J.; Saratale, G.D.; Lo, Y.C.; Chen, W.M.; Tseng, Z.J.; Chang, M.C.; Tsai, B.C.; Sud, A.; Chang, J.S. Simultaneous production of 2,3-butanediol, ethanol and hydrogen with a *Klebsiella* sp. strain isolated from sewage sludge. *Bioresour. Technol.* **2008**, *99*, 7966–7970. [CrossRef]
85. CEPEA. CEPEA/ESALQ Hydrous Ethanol Index (Fuel)—São Paulo State. Available online: <https://cepea.esalq.usp.br/en/indicator/ethanol.aspx> (accessed on 27 June 2023).
86. EPE. Leilões. Available online: <https://www.epe.gov.br/pt/leiloes-de-energia/leiloes> (accessed on 28 June 2023). (In Portuguese)
87. Harahap, B.M.; Ahning, B.K. Acetate Production from Syngas Produced from Lignocellulosic Biomass Materials along with Gaseous Fermentation of the Syngas: A Review. *Microorganisms* **2023**, *11*, 995. [CrossRef]
88. Sauer, M.; Porro, D.; Mattanovich, D.; Branduardi, P. Microbial production of organic acids: Expanding the markets. *Trends Biotechnol.* **2008**, *26*, 100–108. [CrossRef]
89. Angelidaki, I.; Sanders, W. Assessment of the anaerobic biodegradability of macropollutants. *Rev. Environ. Sci. Biotechnol.* **2004**, *3*, 117–129. [CrossRef]
90. EIA. Open Data: Natural Gas. Available online: <https://www.eia.gov/opendata/browser/natural-gas/pri> (accessed on 28 June 2023).
91. Honda. Honda FCEV Concept Makes World Debut at Los Angeles International Auto Show. November 2013. Available online: <https://hondanews.com/en-US/releases/release-47803fbeb894dddb275faf0fb0c0a28-honda-fcev-concept-makes-world-debut-at-los-angeles-international-auto-show> (accessed on 27 June 2023).
92. Peixoto, G.; Pantoja-Filho, J.L.R.; Agnelli, J.A.B.; Barboza, M.; Zaiat, M. Hydrogen and methane production, energy recovery, and organic matter removal from effluents in a two-stage fermentative process. *Appl. Biochem. Biotechnol.* **2012**, *168*, 651–671. [CrossRef] [PubMed]

93. Dias, M.O.S.; Junqueira, T.L.; Cavalett, O.; Cunha, M.P.; Jesus, C.D.F.; Mantelatto, P.E.; Rosell, C.E.V.; Maciel-Filho, R.; Bonomi, A. Cogeneration in integrated first and second generation ethanol from sugarcane. *Chem. Eng. Res. Des.* **2013**, *91*, 1411–1417. [CrossRef]
94. Dantas, G.A.; Legey, L.F.L.; Mazzone, A. Energy from sugarcane bagasse in Brazil: An assessment of the productivity and cost of different technological routes. *Renew. Sustain. Energy Rev.* **2013**, *21*, 356–364. [CrossRef]
95. Clean Cities. *Alternative Fuel Price Report*; U.S. Department of Energy: Washington, DC, USA, 2016. Available online: http://www.afdc.energy.gov/uploads/publication/alternative_fuel_price_report_april_2016.pdf (accessed on 27 June 2023).
96. MOLBASE. Available online: <https://www.molbase.com/> (accessed on 28 June 2023).
97. Chiesa, P.; Macchi, E. A Thermodynamic Analysis of Different Options to Break 60% Electric Efficiency in Combined Cycle Power Plants. *J. Eng. Gas Turbines Power* **2004**, *126*, 770–785. [CrossRef]

Disclaimer/Publisher's Note: The statements, opinions and data contained in all publications are solely those of the individual author(s) and contributor(s) and not of MDPI and/or the editor(s). MDPI and/or the editor(s) disclaim responsibility for any injury to people or property resulting from any ideas, methods, instructions or products referred to in the content.